

Higher-Genus Chen–Gackstatter Surfaces and The Weierstrass Representation for Surfaces of Infinite Genus

Edward C. Thayer

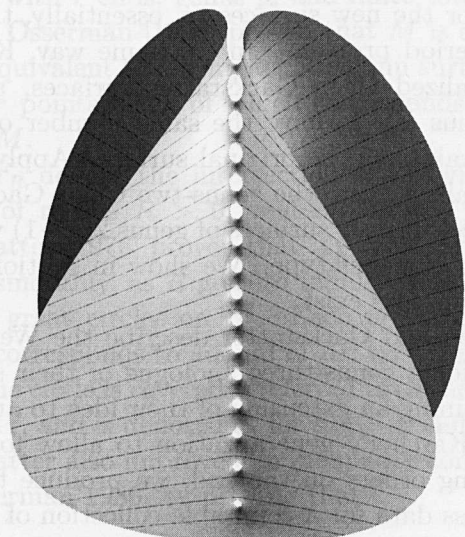
CONTENTS

1. The Chen–Gackstatter Surfaces and Their Generalizations
2. The Weierstrass Representation
3. The General Weierstrass Data and Period Problem for $M_{p,k}$
4. The Examples $M_{2,k}$
5. Numerical Results
6. A Global Representation of Karcher’s Saddle Towers

Acknowledgements

References

Software Availability



Supported by the National Science Foundation under grants DMS-9011083 and DMS-9312087 and by the US Department of Energy under grant DE-FG02-86ER25015 of the Applied Mathematical Science subprogram of the Office of Energy Research.

Chen and Gackstatter [1982] constructed two complete minimal surfaces of finite total curvature, each having one Enneper-type end and all the symmetries of Enneper’s surface. Karcher [1989] generalized the genus-one surface by increasing the winding order of the end. We prove that a similar generalization of the Chen–Gackstatter genus-two surface also exists. We describe a collection of immersed minimal surfaces that generalize both Chen–Gackstatter’s and Karcher’s surfaces by increasing the genus and the winding order of the end. The period problem associated with each of these surfaces is explained geometrically, and we present numerical evidence of its solvability for surfaces of genus as high as 35. We also make conjectures concerning these surfaces, and explain their motivation. Our numerical results led us to the Weierstrass data for several infinite-genus, one-ended, periodic minimal surfaces.

1. THE CHEN–GACKSTATTER SURFACES AND THEIR GENERALIZATIONS

C. C. Chen and F. Gackstatter [1982] constructed immersed minimal surfaces of genus one and two, each having one topological end of Enneper type and the same ambient symmetry group as the classical Enneper surface. These surfaces are illustrated in Figure 1.

We recall that the Enneper surface is given by the Weierstrass data (see Section 2 for definitions)

$$M = \mathbb{C}, \quad g = z, \quad \varphi_3 = dh = z dz.$$

Its symmetry group is generated by two planar reflectional symmetries ($z \rightarrow \bar{z}$ and $z \rightarrow -\bar{z}$ for the Weierstrass data just given) and two rotational symmetries ($z \rightarrow i\bar{z}$ and $z \rightarrow -i\bar{z}$). Each rotational

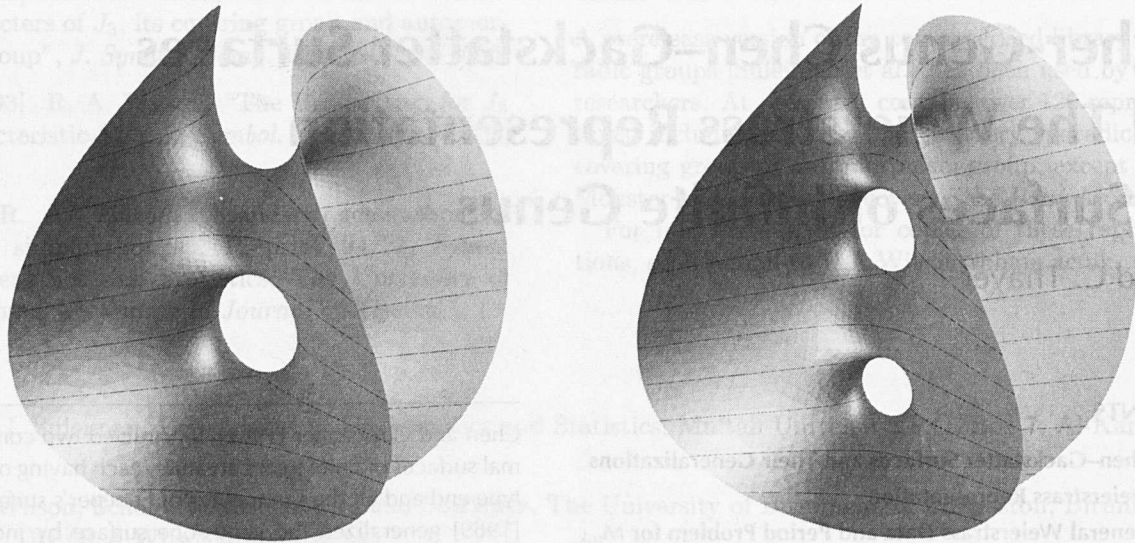


FIGURE 1. Chen and Gackstatter's surfaces of genus one (left) and genus two (right).

symmetry fixes a distinct straight line on the surface ($z = re^{\pm i\pi/4}$), and these lines meet at a single point ($z = 0$) and diverge to the end ($z = \infty$). The composition of the two reflectional symmetries is an orientation-preserving normal rotational symmetry of order two, fixing a line in \mathbb{R}^3 that is perpendicular to the surface and passes through the point $z = 0$.

An end of a minimal surface is said to be of Enneper type if, when the limit normal at the end is vertical, the height differential has a pole of order at least three. Such an end has winding order at least three (see definition in Section 1.1).

Karcher [1989] generalized Chen and Gackstatter's genus-one surface by increasing the order of the normal rotational symmetry from two to arbitrary $k \in \mathbb{N}$ greater than two. This increases the genus from 1 to $k - 1$ and the winding order of the end from 3 to $2k - 1$. This technique of increasing the order of the normal rotational symmetry has led to several new minimal surfaces: see [Hoffman and Meeks 1985; 1988; 1989; 1990; Karcher 1988; 1989], to mention only a few.

As in the case of the Hoffman–Meeks generalization of Costa's three-ended, genus-one surface,

the new surfaces have higher genus, but the period problem does not increase in complexity. This is because the rotational symmetry acts as a cyclic group on the generators of the fundamental group of the new surfaces, thus reducing the period problem for the new surfaces to, essentially, the original period problem. In the same way, Karcher's generalized Chen–Gackstatter surfaces, although of genus $k - 1$, have the same number of period constraints as the original surface. Applying this generalization to the genus-two Chen–Gackstatter surface suggests surfaces of genus $2(k - 1)$ with one end of Enneper type. We show in Section 4 that such surfaces exist.

Chen and Gackstatter describe the Weierstrass data for a genus-three analogue of their surfaces. Combining an extension of their idea to any genus with Karcher's generalization to allow for higher winding orders on the end, we produce the Weierstrass data for a countable collection of surfaces $M_{p,k}$, where $p \geq 0$ and $k \geq 2$ are integers. $M_{p,k}$ has genus $p(k - 1)$, one Enneper-type end of winding order $2k - 1$, the symmetries of Karcher's generalized Enneper surface with the same winding order, and $2p + 1$ finite fixed points of the normal rotational

symmetry. In this notation:

- $M_{0,2}$ is Enneper’s surface;
- $M_{0,k}$ for $k > 2$ are Karcher’s generalizations of Enneper’s surface with winding order $2k - 1$;
- $M_{1,2}$ and $M_{2,2}$ are the Chen–Gackstatter surfaces of genus one and two;
- $M_{1,k}$ with $k > 2$ are Karcher’s generalizations of $M_{1,2}$ with winding order $2k - 1$;
- $M_{2,k}$ with $k > 2$ are generalizations of $M_{2,2}$ with winding order $2k - 1$.

We will refer to these surfaces collectively as CGK surfaces. In Section 3, we describe the Weierstrass data and period problem for $M_{p,k}$, and in Section 5 we present numerical results suggesting that the period problems are solvable for $p \leq 34$, $k \leq 9$. We prove in Section 4 that the period problem in the case $p = 2$ is solvable.

See Figures 2 and 3, as well as the figure on page 19, which represents $M_{15,2}$.

1.1. Conjectures Related to $M_{p,k}$

Let $M \subset \mathbb{R}^3$ be a complete, orientable minimal surface with r ends, genus p , and finite total curvature. Osserman [1986] proved that M is conformally equivalent to a compact Riemann surface \bar{M} minus r points, each of which corresponds to an end of M .

Let Y_R denote the intersection of M with the sphere of radius $R > 0$, centered at the origin. Gackstatter [1976] proved that $X_R := R^{-1}Y_R$ converges smoothly, as R goes to infinity, to a collection of great circles on S^2 . Each of these great circles corresponds to an end of M ; the number of times the circle is covered is referred to as the winding order, and is denoted d_j for the j -th end of M . Gackstatter also improved an inequality contained in [Osserman 1986] by proving that

$$\int_M K dA = 2\pi \left(\chi(\bar{M}) - r - \sum_{j=1}^r d_j \right), \quad (1.1)$$

which was also independently derived in [Jorge and Meeks 1983].

Osserman [1986] showed that if the surface has genus $p = 0$ and $r = 2$, with $d_1 = d_2 = 1$, then M is the catenoid; and that if $p = 0$ and $r = 1$, with $d_1 = 3$, then M is Enneper’s surface $M_{0,2}$. Moreover, it follows from the Strong Halfspace Theorem [Meeks and Rosenberg 1990], without the assumption that the genus is zero, that if $r = 1$ and $d_1 = 1$ then M is the flat plane (see [Kusner 1987] for an alternate proof).

Hoffman [1982] observed that if one maximizes the genus while keeping the total curvature fixed, equation (1.1) implies

$$r + \sum_{j=1}^r d_j = 4,$$

since maximizing genus is equivalent to minimizing $r + \sum d_j$, which is an even integer greater than two. Hence there are only two possibilities for surfaces that maximize genus subject to the constraint of fixed total curvature:

- (i) $r = 1$, with $d_1 = 3$,
- (ii) $r = 2$, with $d_1 = d_2 = 1$.

Schoen [1983] showed that in case (ii) the genus must be zero, corresponding to the catenoid.

Chen and Gackstatter’s surfaces $M_{1,2}$ and $M_{2,2}$ demonstrate that there are surfaces that fall into case (i) and have genus greater than zero. Lopez [1992], and independently Bloß [1989], proved that $M_{1,2}$ is the unique, complete, oriented minimal surface of genus one with total curvature -8π . In particular, maximizing genus with fixed total curvature -8π gives a unique example $M_{1,2}$.

Hoffman and Meeks proposed the following conjecture:

Conjecture 1.1. *Each complete orientable minimal surface with maximal genus p and total curvature $-4\pi(p+1)$ is a Chen–Gackstatter surface $M_{p,2}$, and there are only finitely many surfaces of this type (each corresponding to a distinct period solution).*

For $p \leq 35$, only one solution has ever been found numerically for each surface. The initial work to establish this claim has been to prove the existence

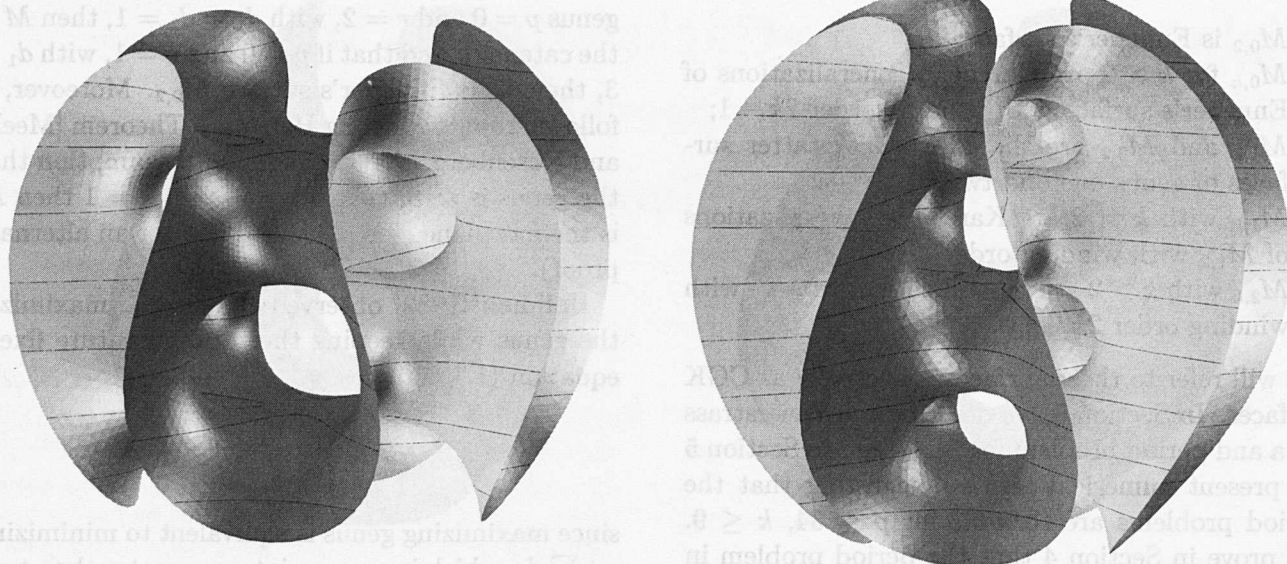


FIGURE 2. Surfaces $M_{1,4}$ (left) and $M_{2,4}$ (right). Compare the original Chen–Gackstatter surfaces in Figure 1, which are called $M_{1,2}$ and $M_{2,2}$ in our notation.

of at least one surface $M_{p,2}$, for each p . We explore this in Section 5.

Evidence gathered from the numerical experiments described in Section 5 suggests the following conjectures:

- Conjecture 1.2.** (i) $M_{p,k}$ exists for all $p \geq 3$, $k \geq 2$.
(ii) Fix the order $k \geq 2$ of the normal rotational symmetry. Let q_1, q_2, \dots, q_p be the strictly positive heights above the origin in \mathbb{R}^3 of the horizontal points of $M_{p,k}$. Rescale each $M_{p,k}$ so that $q_1 = 1$. Then the parameters (q_1, \dots, q_p) that solve the period problems on $M_{p,k}$ converge to the integers as $p \rightarrow \infty$, that is, $\lim_{p \rightarrow \infty} q_j = j$.

The observations that led to these conjectures also led to what we call the *global Weierstrass representation* of some complete periodic minimal surfaces. If $\Sigma \subset \mathbb{R}^3$ is a doubly or singly periodic minimal surface, let Λ be the maximal infinite abelian subgroup generated by its orientation-preserving symmetries. By *global data* for Σ , we mean the Weierstrass data for Σ proper—in other words, the

image of the Weierstrass integral using global Weierstrass data will be the complete surface $\Sigma \subset \mathbb{R}^3$ of infinite total curvature. The classical embedded, periodic surfaces of Scherk viewed globally in \mathbb{R}^3 have one topological end and infinite genus. In general, Callahan, Hoffman, and Meeks [Callahan et al. 1990] proved that any embedded, doubly periodic, complete minimal surface in \mathbb{R}^3 has infinite genus and one topological end. Hence, in order to determine the global data for these examples, one must first understand these rather complicated covering spaces.

Our investigations with $M_{p,k}$ for large p yielded insights into the algebraic structure of some one-ended surfaces of infinite genus. Specifically, we observed that with fixed k , and with the vertical height of the handle on $M_{p,k}$ nearest the straight lines held constant for increasing values of p , in a neighborhood of the origin, $M_{p,k}$ converge to Karcher's singly periodic, symmetric saddle tower with normal rotational symmetry of order k . The saddle towers with normal rotational symmetry of

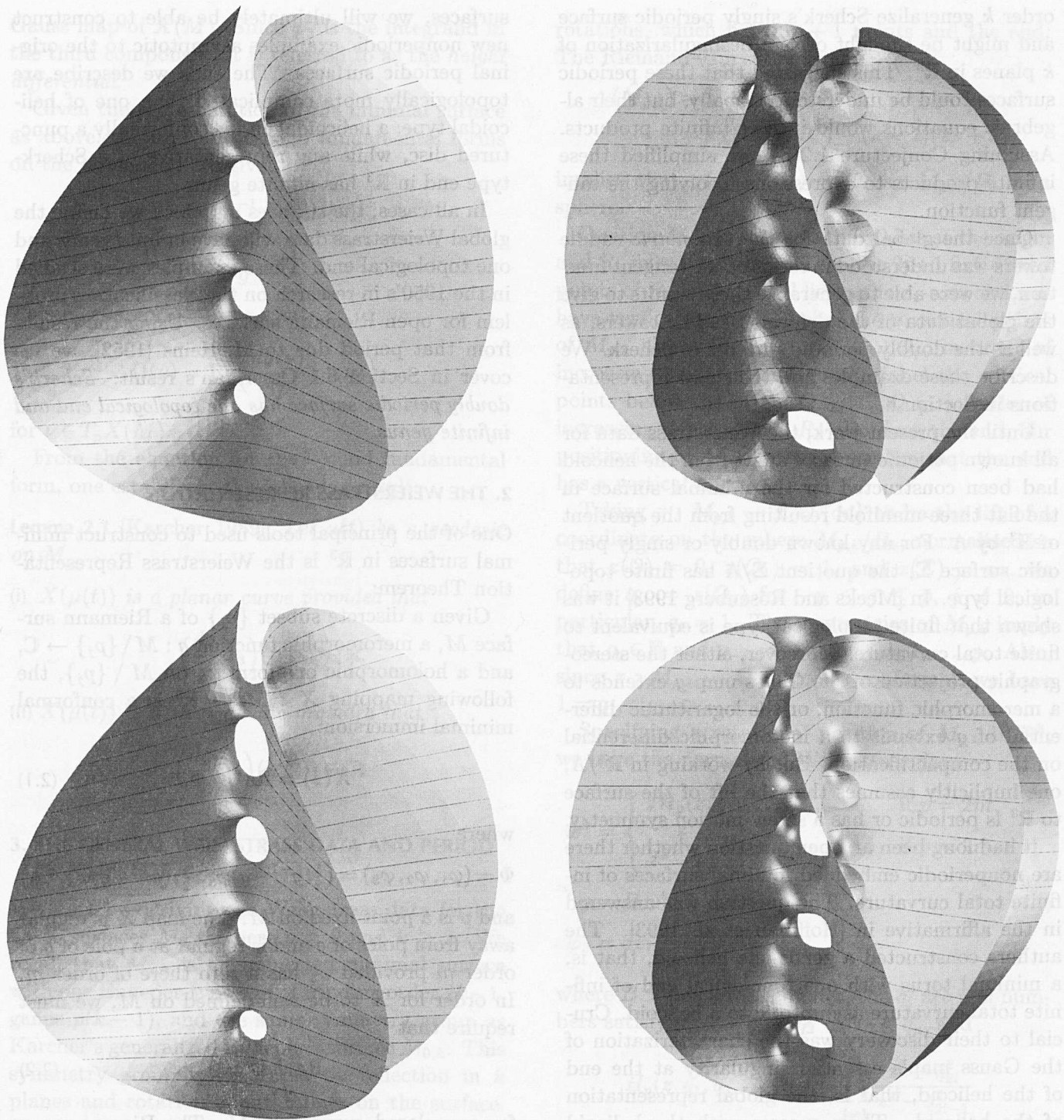


FIGURE 3. Surfaces $M_{3,2}$, $M_{3,4}$, $M_{4,4}$, and $M_{4,2}$ (clockwise from top left).

order k generalize Scherk's singly periodic surface and might be thought of as a desingularization of k planes in \mathbb{R}^3 . This suggested that these periodic surfaces could be understood globally, but their algebraic equations would involve infinite products. Assuming Conjecture 1.2(ii), we simplified these infinite products to expressions involving the tangent function.

Once the global data for the *symmetric* saddle towers was understood in terms of the tangent function, we were able to generalize these results to give the global data of the deformed saddle towers, as well as the doubly periodic surfaces of Scherk. We describe these examples and their new representations in Section 6.

Until the present work, the Weierstrass data for all known periodic surfaces apart from the helicoid had been constructed for the minimal surface in the flat three-manifold resulting from the quotient of \mathbb{R}^3 by Λ . For any known doubly or singly periodic surface Σ , the quotient Σ/Λ has finite topological type. In [Meeks and Rosenberg 1993] it was shown that finite topological type is equivalent to finite total curvature. Moreover, either the stereographic projection of the Gauss map g extends to a meromorphic function, or the logarithmic differential of g extends to a meromorphic differential on the compactification. But by working in \mathbb{R}^3/Λ , one implicitly assumes that the lift of the surface to \mathbb{R}^3 is periodic or has a screw-motion symmetry.

It had long been an open question whether there are nonperiodic embedded minimal surfaces of infinite total curvature. The question was answered in the affirmative in [Hoffman et al. 1993]. The authors constructed a genus-one helicoid, that is, a minimal torus with one topological end of infinite total curvature asymptotic to a helicoid. Crucial to their discovery was the characterization of the Gauss map's essential singularity at the end of the helicoid, that is, the global representation of the helicoid. Their success with the helicoid has produced great interest in characterizing other ends of infinite total curvature. We hope that, by understanding the global data for other periodic

surfaces, we will ultimately be able to construct new nonperiodic examples asymptotic to the original periodic surfaces. The ends we describe are topologically more complicated than one of helicoidal type; a helicoidal end is conformally a punctured disc, while any representative of a Scherk-type end in \mathbb{R}^3 has infinite genus.

In all cases, the surfaces on which we define the global Weierstrass data will have infinite genus and one topological end. These examples were studied in the 1950's in research on the classification problem for open Riemann surfaces. Using the results from that period due to M. Heins [1952], we recover in Section 6.1 Osserman's result: *Scherk's doubly periodic surface has one topological end and infinite genus.*

2. THE WEIERSTRASS REPRESENTATION

One of the principal tools used to construct minimal surfaces in \mathbb{R}^3 is the Weierstrass Representation Theorem:

Given a discrete subset $\{p_j\}$ of a Riemann surface M , a meromorphic function $g : M \setminus \{p_j\} \rightarrow \mathbb{C}$, and a holomorphic one-form φ_3 on $M \setminus \{p_j\}$, the following mapping $X : M \rightarrow \mathbb{R}^3$ is a conformal minimal immersion:

$$X(z) = \operatorname{Re} \int_p^z \Phi, \quad (2.1)$$

where

$$\Phi = (\varphi_1, \varphi_2, \varphi_3) = \left(\frac{1}{2}(g^{-1} - g)\varphi_3, \frac{1}{2}i(g^{-1} + g)\varphi_3, \varphi_3 \right)$$

and p is a point fixed on M . The map X is regular away from poles of g and is regular at a pole of g of order m provided φ_3 has a zero there of order m . In order for X to be well-defined on M , we must require that

$$\operatorname{Re} \oint_\gamma \Phi = 0 \quad (2.2)$$

for any closed curve $\gamma \subset M$. The Riemann surface M , meromorphic function g , and one-form φ_3 are referred to as the *Weierstrass data*. Here, g is the stereographic projection from $(0, 0, 1)$ of the

Gauss map of $X(M)$. Since φ_3 is the integrand in the third component, it is referred to as the *height differential*.

Given the representation of the minimal surface as above, the first and second fundamental forms on the immersion are given by

$$\begin{aligned} I &= \frac{1}{4}(|g|^{-1} + |g|)^2 |\varphi_3|^2 \\ II &= \operatorname{Re}\left(\frac{dg}{g} \varphi_3\right). \end{aligned}$$

This means, for example, that

$$II(\nu) = \operatorname{Re}\left(\frac{dg(\nu)}{g(p)} \varphi_3(\nu)\right),$$

for $\nu \in T_p X(M)$.

From the equation for the second fundamental form, one establishes the following result:

Lemma 2.1 [Karcher 1989]. *Let $\mu(t)$ be a geodesic on M .*

(i) $X(\mu(t))$ is a planar curve provided that

$$\left(\frac{dg}{g} \varphi_3\right)(\mu'(t)) \in \mathbb{R}$$

(ii) $X(\mu(t))$ is a straight line provided that

$$\left(\frac{dg}{g} \varphi_3\right)(\mu'(t)) \in i\mathbb{R}.$$

3. THE GENERAL WEIERSTRASS DATA AND PERIOD PROBLEM FOR $M_{p,k}$

We start by deriving the Weierstrass data for the CGK surfaces $M_{p,k}$, where $p \geq 0$ and $k \geq 2$. We recall that $M_{p,k}$ is an immersed minimal surface with one Enneper-type end of winding order $2k - 1$, genus $p(k - 1)$, and the same symmetry group as Karcher’s generalized Enneper’s surface $M_{0,k}$. This symmetry group is generated by reflection in k planes and rotation about k lines on the surface. The lines meet at a single point \mathcal{O} on the surface and pass through the end, which is represented by a point $E \in \bar{M}_{p,k}$. The reflectional symmetries generate a cyclic subgroup R_k of order k , consisting of

rotations, which fixes $2p + 1$ points and the end. The Riemann–Hurwitz formula

$$\begin{aligned} \chi(\bar{M}_{p,k}) &= 2 - 2p(k - 1) \\ &= k\chi(\bar{M}_{p,k}/R_k) - (k - 1)(2p + 2) \end{aligned}$$

implies that $\chi(\bar{M}_{p,k}/R_k) = 2$, so $\bar{M}_{p,k}/R_k$ is a sphere.

Position $M_{p,k}$ in space so that \mathcal{O} lies at the origin and R_k fixes the x_3 -axis. Then the $2p + 1$ finite fixed points of R_k on $M_{p,k}$ will lie on the x_3 -axis and will have vertical normals. Label the p vertical points of $M_{p,k}$ above the origin Q_1, \dots, Q_p , in order of increasing height. Analogously, label the vertical points below the origin Q_{-1}, \dots, Q_{-p} , in order of increasing depth. Since R_k also fixes the end, our positioning of $M_{p,k}$ in space implies that the end has a vertical normal.

Taking $z : M_{p,k} \rightarrow \mathbb{C} \cup \{\infty\}$ to be the lift of a coordinate on the sphere $M_{p,k}/R_k$, normalized so that $z(\mathcal{O}) = 0$, $z(Q_1) = 1$, and $z(E) = \infty$, we define $q_j := z(Q_j)$ for $-p \leq j \leq p$, $j \neq 0$; in particular, $q_1 = 1$. The symmetries of $M_{p,k}$ imply that $q_j \in \mathbb{R}$ and $q_{-j} = -q_j$ for $j = 1, \dots, p$. Also, since $z : M_{p,k} \rightarrow \mathbb{C} \cup \{\infty\}$ is conformal, we have $1 = q_1 < q_2 < \dots < q_p$.

Specifying a rotational position of $M_{p,k}$ in \mathbb{R}^3 , we have the normalized Weierstrass data

$$\begin{aligned} w^k &= \begin{cases} zH_p(z, q_1, \dots, q_p), & \text{if } p = 2m, \\ \frac{z}{z^2 - q_p^2} H_p(z, q_1, \dots, q_p) & \text{if } p = 2m + 1, \end{cases} \\ g &= B w^{k-1}, \\ \varphi_3 &= dz, \end{aligned} \tag{3.1}$$

where $B > 0$ is a real number, the q_j are real numbers satisfying $1 = q_1 < q_2 < \dots < q_p$, and

$$H_p(z, q_1, q_2, \dots, q_p) = \prod_{l=1}^m \frac{z^2 - q_{2l}^2}{z^2 - q_{2l-1}^2}.$$

To summarize what is known about the $M_{p,k}$:

(i) The $M_{0,k}$ are genus-zero generalizations of Enneper’s surface with winding order $2k - 1$.

- (ii) $M_{1,2}$ and $M_{2,2}$ are the original surfaces discovered by Chen and Gackstatter, of genus one and two.
- (iii) Karcher [1989] extended Chen and Gackstatter's original existence proof of $M_{1,2}$ to prove $M_{1,k}$ exists for $k > 2$.
- (iv) In Section 4, we show that Chen and Gackstatter's existence proof for $M_{2,2}$ can be modified to give the existence of $M_{2,k}$ for $k > 2$.
- (v) Espírito Santo [1993] proved that $M_{3,2}$ exists by estimating the path integrals involved in the period problem using Riemann sums.
- (vi) In general, $M_{p,k}$ has genus $p(k - 1)$, and by the Jorge–Meeks–Gackstatter equality, its total curvature is

$$-4\pi(\text{genus} - k + 1) = -4\pi(p - 1)(k - 1).$$

3.1. The General Period Problem

Given the Weierstrass data (3.1), the minimal surface $X : M_{p,k} \rightarrow \mathbb{R}^3$ given by

$$X(q) = \text{Re} \int_{q_0}^q \Phi \tag{3.2}$$

(where $q_0 \in M_{p,k}$ is fixed) and

$$\Phi = \begin{pmatrix} \varphi_1 \\ \varphi_2 \\ \varphi_3 \end{pmatrix} = \begin{pmatrix} \frac{1}{2}(g^{-1} - g)\varphi_3 \\ i\frac{1}{2}(g^{-1} + g)\varphi_3 \\ \varphi_3 \end{pmatrix}$$

is well-defined, provided that $\oint_\gamma \Phi \in i\mathbb{R}$ for γ any closed curve on $M_{p,k}$. Since $\varphi_3 = dz$ is an exact form, $\oint_\gamma \varphi_3 = 0$ for any closed curve γ , so we need only be concerned with the first and second components of the mapping X . Determining the values of B, q_2, q_3, \dots, q_p in such a way that this condition is satisfied is referred to as solving the *period problem*.

The symmetries of $M_{p,k}$ simplify the period problem significantly, reducing the expected number of homotopy classes to be considered from $2p(k - 1)$ to p . Choosing representatives γ_j , for $-p \leq j \leq p$, $j \neq 0$, as in Figure 4, we will see that we need only check the periods of the first or second components of X along the curves $\gamma_1, \gamma_2, \dots, \gamma_p$.

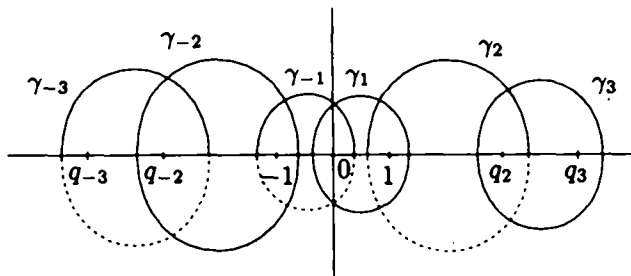


FIGURE 4. Values of z with homotopy class representatives indicated. The change from dotted lines to solid lines indicates that the curve changes sheets on $M_{p,k}$.

Recall that generically we have positioned $M_{p,k}$ in such a way that 0 lies at the origin and the points Q_j are horizontal. Additionally, our choice of B in (3.1) positions $M_{p,k}$ so that the planar curve corresponding to $z \in [0, 1]$ and $w \in \mathbb{R}$ lies in the $x_2 = 0$ plane.

While one may write out each of the curves γ_j and examine their periods, we prefer to present a more geometric description of these periods. We start by considering the image of one sheet of w under the mapping X defined in (3.2), where w is restricted to vary over one sheet, say the sheet where the phase of w lies between $-\pi/k$ and π/k . This portion of $M_{p,k}$ is bounded by planar curves and contains two horizontal rays starting at the origin and passing to the end. If the period problem were solved, the planar curves would lie in either of two planes, both of which contain the x_3 -axis and make an angle of π/k with the plane $x_2 = 0$. See Figure 5 (bottom right). Since $M_{p,k}$ is symmetric about the straight rays emanating from 0 , once the planar curves above the origin lie in the appropriate planes through the origin, the curves below the origin will also. Hence we need only consider the periods around $\gamma_1, \dots, \gamma_p$.

Each γ_j is homotopic to a piecewise smooth curve made up of two smooth planar curves joined at horizontal points on the surface, with the angle between the planes in which these curves lie being equal to π/k . The two constituent smooth planar curves, moreover, are congruent by a reflectional

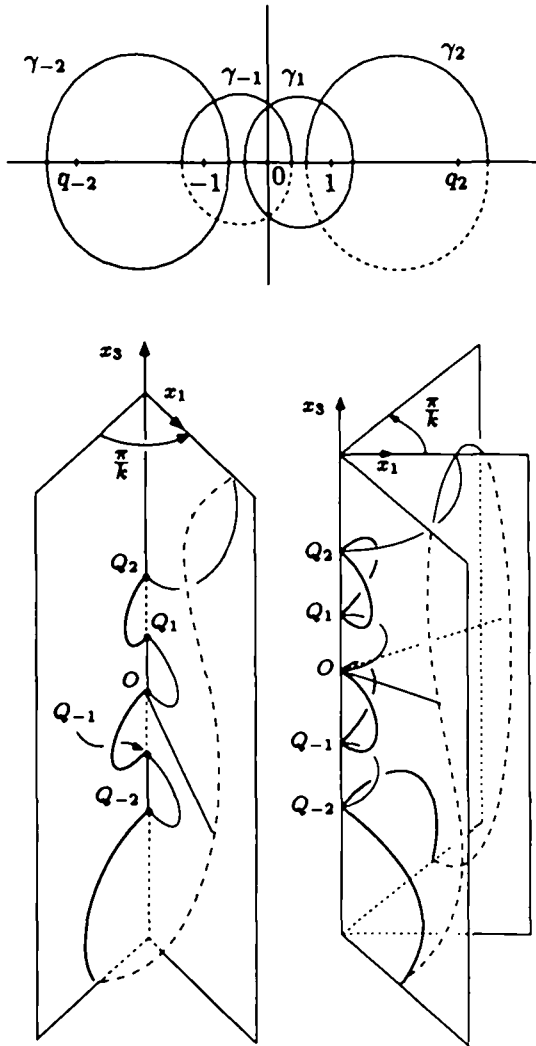


FIGURE 5. Three views of $M_{2,k}$ once the periods have been solved. : Top: z -plane with homotopy classes on $M_{2,k}$. Bottom left: sketch of the boundary curves of $M_{2,k}$ in \mathbb{R}^3 corresponding to z such that $\text{Im}(z) \geq 0$ and w lies on one sheet. Bottom right: the same boundary curves after reflection through the $x_2 = 0$ plane.

symmetry. We modify our notation so that γ_j refers to this piecewise smooth curve. Hence

$$\text{Re} \oint_{\gamma_j} (\varphi_1, \varphi_2) = 2 \text{Re} \int_{z=q_{j-1}}^{z=q_j} (\varphi_1, \varphi_2),$$

for $j = 1, 2, \dots, p$, where w is restricted so that the phase of w lies between $-\pi/k$ and π/k .

Our normalization of the Weierstrass data ensures that the planar curve joining O and Q_1 lies in the $x_2 = 0$ plane, so that

$$\text{Re} \oint_{\gamma_1} \varphi_2 = 2 \text{Re} \int_{z=0}^{z=1} \varphi_2 = 0.$$

Hence we need only consider $\text{Re} \oint_{\gamma_1} \varphi_1$.

A careful examination of the other periods reveals a similar simplification is possible for them too. In particular, γ_2 starts at the point Q_1 , climbs to Q_2 , and lies in a vertical plane parallel to a plane rotated $\pm\pi/k$ from the $x_2 = 0$ plane. The real parts of the periods about γ_2 are zero when Q_2 lies on the x_3 -axis, which is true when the second component of Q_2 is zero. Therefore, provided that

$$\text{Re} \int_{z=0}^{z=1} (\varphi_1, \varphi_2) = 0,$$

it is sufficient to know that

$$\text{Re} \int_{z=1}^{z=q_2} \varphi_2 = 0$$

to ensure that the real parts of the periods about γ_2 are zero.

In a similar fashion, we may now argue that the conditions

$$\text{Re} \oint_{\gamma_3} (\varphi_1, \varphi_2) = 0 \quad \text{and} \quad \text{Re} \oint_{\gamma_4} (\varphi_1, \varphi_2) = 0$$

are satisfied, provided that

$$\text{Re} \int_{z=q_2}^{z=q_3} \varphi_1 = 0 \quad \text{and} \quad \text{Re} \int_{z=q_3}^{z=q_4} \varphi_2 = 0.$$

In general, the period problem reduces to showing that

$$\begin{aligned} \text{Re} \int_{z=q_{j-1}}^{z=q_j} \varphi_1 &= 0 \quad \text{for } j \text{ odd,} \\ \text{Re} \int_{z=q_{j-1}}^{z=q_j} \varphi_2 &= 0 \quad \text{for } j \text{ even.} \end{aligned} \tag{3.3}$$

Although this period problem involves finding the zero of a function $\Omega : \mathbb{R}^p \rightarrow \mathbb{R}^p$, which is generically difficult, more can be said. In fact, an observation in [Chen and Gackstatter 1982] generalizes

to this case and allows us to determine the value of B , given the values of q_2, q_3, \dots, q_p such that the first of these period conditions is satisfied. That is,

$$\operatorname{Re} \int_{z=0}^{z=1} \varphi_1 = \operatorname{Re} \int_0^1 \left(\frac{1}{Bw^{k-1}} - Bw^{k-1} \right) dz = 0$$

provided that

$$B^2 = \operatorname{Re} \frac{\int_0^1 dz/w^{k-1}}{\int_0^1 w^{k-1} dz}. \tag{3.4}$$

One must confirm that the right hand side is positive, since we need $B \in \mathbb{R}$, $B \neq 0$; this is immediate since w is a strictly decreasing negative real-valued function for $z \in (0, 1)$, as seen from equation (3.1). Hence the first period condition imposes a constraint on B , given the values q_2, \dots, q_p .

One typically looks to degree-theory arguments when searching for zeros of functions $\Omega : \mathbb{R}^{p-1} \rightarrow \mathbb{R}^{p-1}$, and this approach has been successful for period problems arising from other minimal surfaces [Wohlgemuth 1993; Traizet]. Known zeros, representing lower-genus examples, severely complicate these methods in the present case. Specifically, the boundary of the domain $1 < q_2 < \dots < q_p$, over which one searches, contains known zeros for the period functions. For example, if, while searching for the solution to the period problem for $M_{3,2}$, we encounter $q_j = q_l$ for $j \neq l$, the solution found corresponds to a solution of the period problem for $M_{2,2}$. Should several parameters coalesce, the surface may actually degenerate to Enneper's surface $M_{0,2}$.

4. THE EXAMPLES $M_{2,k}$

In this section we solve the period problem for the new surfaces $M_{2,k}$, where $k \geq 3$. The proof presented is an extension of the original proof given by Chen and Gackstatter for $M_{2,2}$, with the substitution of the more general Weierstrass data and some additional observations.

Recall from (3.1) that the Weierstrass data for $M_{2,k}$ is

$$\begin{aligned} w^k &= \frac{z(z^2 - q_2^2)}{(z^2 - 1)}, \\ g &= Bw^{k-1}, \\ \eta &= dz, \end{aligned} \tag{4.1}$$

where $B > 0$ and $q_2 > 1$ are reals. The general period problem (3.3) for $M_{p,k}$ reduces to the following two-dimensional problem:

Period Problem. Show there exist $B > 0$ and $q_2 > 1$ such that:

$$\operatorname{Re} \int_0^1 \frac{1}{2} \left(\frac{1}{Bw^{k-1}} - Bw^{k-1} \right) dz = 0$$

and

$$\operatorname{Re} \int_1^{q_2} \frac{i}{2} \left(\frac{1}{Bw^{k-1}} + Bw^{k-1} \right) dz = 0.$$

Denoting the real k -th root of a positive real number r by $\sqrt[k]{r}$, we see that, for $z \in (0, 1)$,

$$w^{k-1} = \sqrt[k]{\left(\frac{z(z^2 - q_2^2)}{z^2 - 1} \right)^{k-1}},$$

and for $z \in (1, q_2)$,

$$w^{k-1} = e^{i\pi(k-1)/k} \sqrt[k]{\left(\frac{z(q_2^2 - z^2)}{z^2 - 1} \right)^{k-1}}.$$

For convenience we define the following quantities:

$$F_1 = \int_0^1 \sqrt[k]{\left(\frac{z(z^2 - q_2^2)}{z^2 - 1} \right)^{k-1}} dz;$$

$$G_1 = \int_0^1 \sqrt[k]{\left(\frac{z^2 - 1}{z(z^2 - q_2^2)} \right)^{k-1}} dz;$$

$$F_2 = \int_1^{q_2} \sqrt[k]{\left(\frac{z(q_2^2 - z^2)}{z^2 - 1} \right)^{k-1}} dz;$$

$$G_2 = \int_1^{q_2} \sqrt[k]{\left(\frac{z^2 - 1}{z(q_2^2 - z^2)} \right)^{k-1}} dz.$$

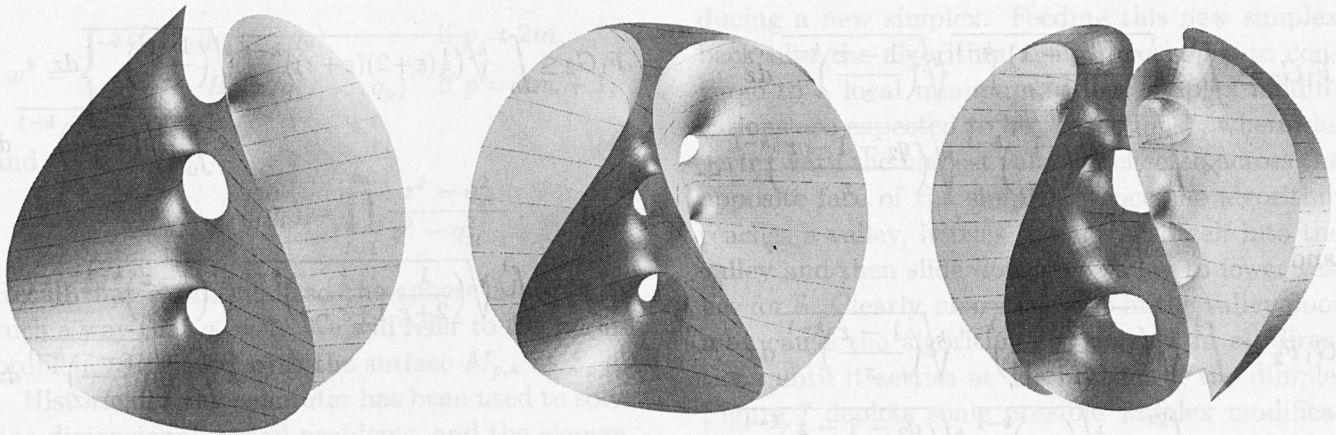


FIGURE 6. Genus-two surface of Chen and Gackstatter (left), and generalizations $M_{2,k}$: in the middle, $k = 3$ (winding order 5), and on the right, $k = 4$ (winding order 7).

With them, the equations in the two-dimensional period problem become

$$\frac{1}{2B}G_1 - \frac{B}{2}F_1 = 0$$

and

$$\frac{1}{2B}\operatorname{Re}(ie^{-i\pi(k-1)/k})G_2 + \frac{B}{2}\operatorname{Re}(ie^{i\pi(k-1)/k})F_2 = 0,$$

which we can rewrite as

$$G_1 = B^2F_1 \quad \text{and} \quad G_2 = B^2F_2$$

or, equivalently,

$$G_1 = B^2F_1, \quad (4.2)$$

$$G_1F_2 = F_1G_2. \quad (4.3)$$

As we observed in the discussion of the general period problem, F_1 and G_1 are nonzero and have the same sign, so (4.2) determines B , for any q_2 . Hence we need only find a value of q_2 for which (4.3) is valid.

We will show that $G_1F_2 \leq F_1G_2$ for q_2 sufficiently large, and that $G_1F_2 \geq F_1G_2$ for q_2 very near 1. Then, by the intermediate value theorem, a value of $q_2 > 1$ exists such that (4.3) holds.

Applying several changes of variables, we have

$$F_1 = \int_0^1 \sqrt[k]{\left(\frac{(q_2-1+z)(q_2+1-z)}{2-z}\right)^{k-1}} \sqrt[k]{\left(\frac{1-z}{z}\right)^{k-1}} dz$$

$$G_1 = \int_0^1 \sqrt[k]{\left(\frac{1+z}{(q_2+z)(q_2-z)}\right)^{k-1}} \sqrt[k]{\left(\frac{1-z}{z}\right)^{k-1}} dz$$

$$F_2 = \int_0^{q_2-1} \sqrt[k]{\left(\frac{(1+z)(z+1+q_2)}{2+z}\right)^{k-1}} \sqrt[k]{\left(\frac{q_2-1-z}{z}\right)^{k-1}} dz$$

$$G_2 = \int_0^{q_2-1} \sqrt[k]{\left(\frac{q_2-z+1}{(q_2-z)(2q_2-z)}\right)^{k-1}} \sqrt[k]{\left(\frac{q_2-1-z}{z}\right)^{k-1}} dz$$

By using the bounds on the values of z over which each term is integrated, we get

$$F_1 \geq \int_0^1 \sqrt[k]{\left(\frac{q_2(q_2-1)}{2}\right)^{k-1}} \sqrt[k]{\left(\frac{1-z}{z}\right)^{k-1}} dz,$$

$$G_1 \leq \int_0^1 \sqrt[k]{\left(\frac{2}{q_2(q_2-1)}\right)^{k-1}} \sqrt[k]{\left(\frac{1-z}{z}\right)^{k-1}} dz,$$

$$F_2 \leq \int_0^{q_2-1} \sqrt[k]{(2q_2)^{k-1}} \sqrt[k]{\left(\frac{q_2-1-z}{z}\right)^{k-1}} dz,$$

$$G_2 \geq \int_0^{q_2-1} \sqrt[k]{\left(\frac{1}{2q_2}\right)^{k-1}} \sqrt[k]{\left(\frac{q_2-1-z}{z}\right)^{k-1}} dz.$$

Hence

$$F_1 G_2 \geq \int_0^1 \sqrt[k]{\left(\frac{q_2(q_2-1)}{2}\right)^{k-1}} \sqrt[k]{\left(\frac{1-z}{z}\right)^{k-1}} dz \\ \times \int_0^{q_2-1} \sqrt[k]{\left(\frac{1}{2q_2}\right)^{k-1}} \sqrt[k]{\left(\frac{q_2-1-z}{z}\right)^{k-1}} dz$$

and

$$G_1 F_2 \leq \int_0^1 \sqrt[k]{\left(\frac{2}{q_2(q_2-1)}\right)^{k-1}} \sqrt[k]{\left(\frac{1-z}{z}\right)^{k-1}} dz \\ \times \int_0^{q_2-1} \sqrt[k]{(2q_2)^{k-1}} \sqrt[k]{\left(\frac{q_2-1-z}{z}\right)^{k-1}} dz.$$

For $q_2 > 1$ sufficiently large we have

$$\sqrt[k]{\left(\frac{2}{q_2-1}\right)^{k-1}} \leq \sqrt[k]{\left(\frac{q_2-1}{2}\right)^{k-1}}$$

Hence $G_1 F_2 \leq F_1 G_2$ for these values.

On the other hand, writing $q_2 = 1 + \varepsilon$,

$$F_1 = \int_0^1 \sqrt[k]{\left(\frac{(\varepsilon+z)(2+\varepsilon-z)}{2-z}\right)^{k-1}} \sqrt[k]{\left(\frac{1-z}{z}\right)^{k-1}} dz \\ \leq \int_0^1 \sqrt[k]{\left(\frac{\varepsilon+2}{2}(\varepsilon+z)\right)^{k-1}} \sqrt[k]{\left(\frac{1-z}{z}\right)^{k-1}} dz, \\ G_1 = \int_0^1 \sqrt[k]{\left(\frac{1+z}{(1+\varepsilon+z)(1+\varepsilon-z)}\right)^{k-1}} \sqrt[k]{\left(\frac{1-z}{z}\right)^{k-1}} dz \\ \geq \int_0^1 \sqrt[k]{\left(\frac{1}{2+\varepsilon} \frac{1}{1+\varepsilon-z}\right)^{k-1}} \sqrt[k]{\left(\frac{1-z}{z}\right)^{k-1}} dz, \\ F_2 = \int_0^\varepsilon \sqrt[k]{\left(\frac{(1+z)(z+2+\varepsilon)}{2+z}\right)^{k-1}} \sqrt[k]{\left(\frac{\varepsilon-z}{z}\right)^{k-1}} dz \\ \geq \int_0^\varepsilon \sqrt[k]{\left(\frac{\varepsilon-z}{z}\right)^{k-1}} dz, \\ G_2 = \int_0^\varepsilon \sqrt[k]{\left(\frac{2+\varepsilon-z}{(1+\varepsilon-z)(2+2\varepsilon-z)}\right)^{k-1}} \sqrt[k]{\left(\frac{\varepsilon-z}{z}\right)^{k-1}} dz \\ \leq \int_0^\varepsilon \sqrt[k]{\left(\frac{\varepsilon-z}{z}\right)^{k-1}} dz.$$

Therefore

$$F_1 G_2 \leq \int_0^1 \sqrt[k]{\left(\frac{1}{2}(\varepsilon+2)(\varepsilon+z)\right)^{k-1}} \sqrt[k]{\left(\frac{1-z}{z}\right)^{k-1}} dz \\ \times \int_0^\varepsilon \sqrt[k]{\left(\frac{\varepsilon-z}{z}\right)^{k-1}} dz$$

and

$$G_1 F_2 \geq \int_0^1 \sqrt[k]{\left(\frac{1}{2+\varepsilon} \frac{1}{1+\varepsilon-z}\right)^{k-1}} \sqrt[k]{\left(\frac{1-z}{z}\right)^{k-1}} dz \\ \times \int_0^\varepsilon \sqrt[k]{\left(\frac{\varepsilon-z}{z}\right)^{k-1}} dz.$$

For $\varepsilon > 0$ sufficiently small,

$$\sqrt[k]{\left(\frac{1}{2+\varepsilon} \frac{1}{1+\varepsilon-z}\right)^{k-1}} \geq \sqrt[k]{\left(\frac{\varepsilon+2}{2}(\varepsilon+z)\right)^{k-1}}$$

Hence $G_1 F_2 \geq F_1 G_2$ for such values of $\varepsilon = q_2 - 1$.

We have shown that there exist values for $B > 0$ and $q_2 > 1$ for which both (4.2) and (4.3) hold; therefore the two-dimensional period problem associated to $M_{2,k}$ can be solved for $k \geq 3$. In other words, $M_{2,k}$ exists:

Theorem 4.1. *For each integer $k \geq 3$, there exists an immersed minimal surface of genus $2(k-1)$ with one generalized Enneper-type end of winding order $2k-1$.*

5. NUMERICAL RESULTS

Researchers in minimal surface theory often have used the computer to search for numerical solutions to the period problem. In this section we describe work on the period problem for the general CGK surfaces $M_{p,k}$ given by (3.3). More precisely, we want to find a zero for the function $\Omega = (\Omega_1, \dots, \Omega_p) : \mathbb{R}^p \rightarrow \mathbb{R}^p$ with components

$$\Omega_j(B, q_2, q_3, \dots, q_p) = \begin{cases} \operatorname{Re} \int_{z=q_{j-1}}^{z=q_j} \frac{1}{2}(g^{-1} - g) dz & \text{if } j \text{ is odd,} \\ \operatorname{Re} \int_{z=q_{j-1}}^{z=q_j} \frac{1}{2}(g^{-1} + g) dz & \text{if } j \text{ is even,} \end{cases} \quad (5.1)$$

where $g = B w^{k-1}$,

$$w^k = \begin{cases} z H_p(z, q_1, \dots, q_p) & \text{if } p = 2m, \\ \frac{z}{z^2 - q_p^2} H_p(z, q_1, \dots, q_p) & \text{if } p = 2m + 1, \end{cases}$$

and

$$H_p(z, q_1, \dots, q_p) = \prod_{l=1}^m \frac{z^2 - q_{2l}^2}{z^2 - q_{2l-1}^2}$$

Recall that we normalized the sphere $M_{p,k}/R_k$ in such a way that $q_1 = 1$. We will refer to the period problem associated with the surface $M_{p,k}$ as $S_{p,k}$.

Historically, the computer has been used to solve one-dimensional period problems, and the elementary bisection method was adequate in these cases. Providing the bisection method with an interval in which a zero is thought to be found, the algorithm evaluates the function at the endpoints, and based on these values it bisects the interval until a zero is approached. But since we intended to consider period problems of arbitrary dimension and zeros can not be bracketed in higher dimensions, we sought an algorithm that would generalize to higher dimensions more easily.

In searching for such an algorithm, we considered several numerical methods designed to find the minimum of a function $\mathcal{S} : \mathbb{R}^p \rightarrow \mathbb{R}$. Taking

$$\mathcal{S}(B, q_2, q_3, \dots, q_p) := \sum_{j=1}^p \Omega_j^2(B, q_2, q_3, \dots, q_p),$$

we change the problem from one of finding a zero to one of finding a minimum for this new non-negative function, in the hope that the minimum value is zero. Additionally, since each evaluation of the functions Ω_j involves integral calculations, we sought algorithms that did not require computation of the partial derivatives of \mathcal{S} .

The algorithm we chose was the downhill simplex method in multidimensions [Nelder and Mead 1965] (see also [Press et al. 1986, pp. 289–293]). It starts with an initial simplex in \mathbb{R}^p , near which one expects to find a zero for \mathcal{S} . By comparing the value of \mathcal{S} on the vertices of this simplex, the algorithm moves one or more vertices “downhill”

toward lower values of the function, thereby producing a new simplex. Feeding this new simplex back into the algorithm again, one hopes to converge to a local minimum. Most simplex modifications are expected to be “reflections”, where the vertex with the highest value is reflected across the opposite face of the simplex. Once the algorithm reaches a valley, it tries to contract itself into the valley and then slide down the valley to lower values for \mathcal{S} . Clearly, sharp dimples in the valley floor may cause the algorithm to contract in all directions until it settles at the bottom of the dimple. Figure 7 depicts some possible simplex modifications resulting from one iteration of the method.

To simplify the input of the initial data for this algorithm, we generate our simplices by constructing p other vertices, $x_j = x_0 + \epsilon e_j$, from a single point $x_0 \in \mathbb{R}^p$, where (e_1, e_2, \dots, e_p) is the standard basis for \mathbb{R}^p . The initial simplex is then the one whose vertices are x_0, x_1, \dots, x_p .

We tested the algorithm (and our code) by considering the original surfaces $M_{1,2}$ and $M_{2,2}$ proved to exist by Chen and Gackstatter. The numerical solutions found for these surfaces turned out to be correct, so we started searching for solutions to the period problem $S_{3,2}$ associated to $M_{3,2}$, which was not known to exist at the time of the computation. After finding the solution to this three-dimensional period problem, we moved on to the four-dimensional problem for $S_{4,2}$, and ultimately continued this process by searching for solutions to $S_{p+1,2}$ once we had the solutions for $S_{p,2}$. We stopped doing computer searches once we reached $p = 34$. Two of the solutions are illustrated in Figure 8.

It is important to keep in mind that each new period problem $S_{p,2}$ required an initial simplex, or at least an initial point, in \mathbb{R}^p , to get the search algorithm started. As p became large, it became more and more difficult to find such initial data; from random initial data, the algorithm tended to converge to degenerate solutions (those where two or more q_j 's coincided). If, on the other hand, the initial guess was near enough to a nondegenerate

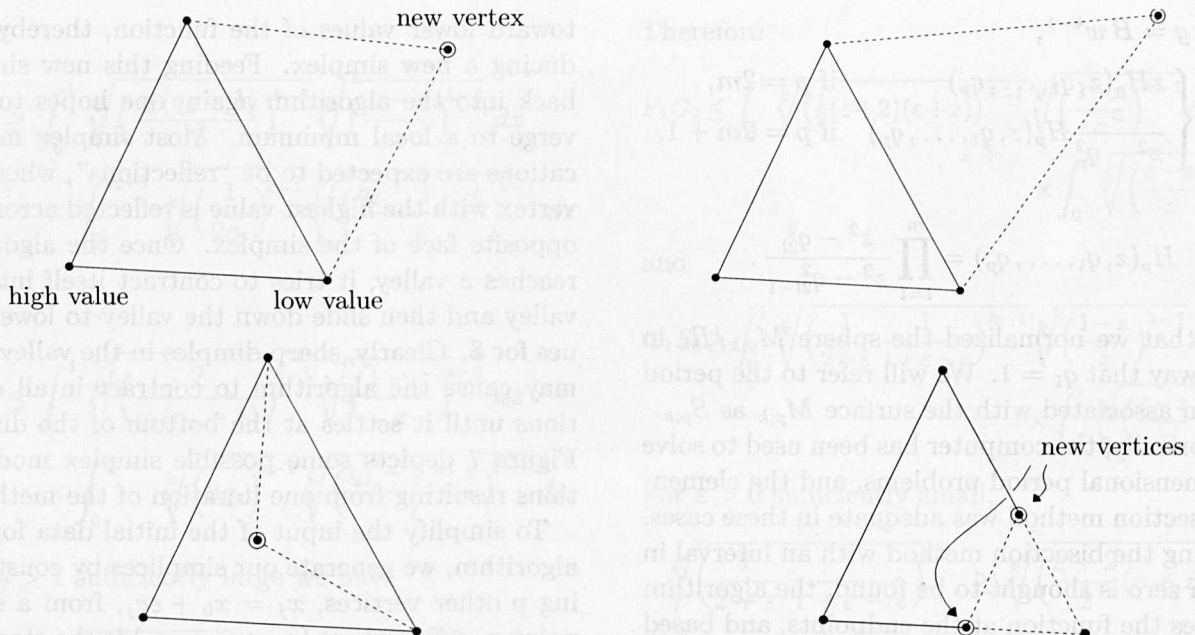


FIGURE 7. Possible modifications of a two-dimensional simplex during one step of the downhill simplex method. The initial simplex is drawn with solid lines while the modified simplex has dashed lines and can be either reflected away from a high point (top left), reflected and expanded (top right), contracted in one dimension away from a high point (bottom left), or contracted along all directions towards a low point (bottom right).

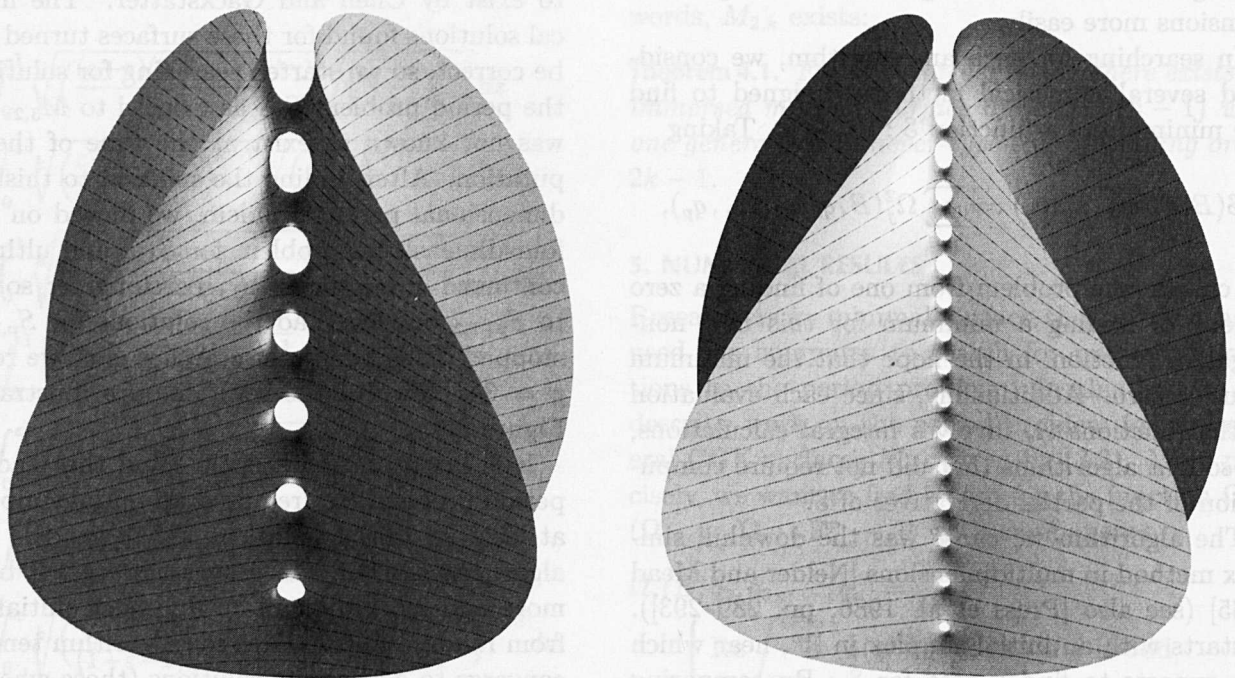


FIGURE 8. Images of $M_{6,2}$ (left) and $M_{15,2}$ (right) made from numerical approximations of the associated six-dimensional and fifteen-dimensional period problems.

solution, the algorithm easily converged to these solutions. At that point we started looking for information that might allow us to predict where in \mathbb{R}^p a solution might be found for $S_{p,2}$. Surprisingly, we found some good predictors.

The most productive idea was to return to the original Weierstrass data and choose another normalization for the coordinate z on $M_{p,2}/R_2$. Instead of choosing z so that $z(Q_1/R_2) = 1$, we choose z so that the branch point for the Gauss map occurs at a specific point along the imaginary axis, which has a net effect of setting B constant at 1. Geometrically, this new normalization corresponds to a homothety of the surface $M_{p,2} \subset \mathbb{R}^3$. Instead of viewing the component period functions Ω_j as functions of B, q_2, \dots, q_p , we now view them as functions of q_1, q_2, \dots, q_p . Using this normalization, we generated the table of solutions to $S_{p,2}$ found in Figure 9 (top), where each horizontal line corresponds to a distinct value of p and the tick marks denote the values of the q_j 's solving $S_{p,2}$.

The patterns found in tables of this form for solutions of $S_{p,2}$ for $p < 9$ allowed us to predict where the next solution might be found. Although we have no explanation at this point for the obvious pairing of the values q_j and q_{j+1} , nor for the general “curves” seen in this data, it is our opinion that, without these observations, searches in \mathbb{R}^p for solutions to $S_{p,2}$ with $p > 10$ would mostly yield degenerate solutions.

Soon after making these calculations, we started on the generic problem $S_{p,k}$. To our surprise, the solutions for $S_{p,2}$ were very near nondegenerate solutions for $S_{p,k}$ for k near 2, and for larger k , the nearest known solution generally served as an excellent initiator. Using this observation, we have found solutions to $S_{p,k}$ for $p < 35$ and $k < 10$.

Returning to the original normalization for the coordinate z on the sphere $M_{p,k}/R_k$, and transforming the solutions of $S_{p,k}$ to reflect this other normalization, we produced the data in Figure 9 (bottom). Here the first patterns are less obvious, but another one emerges. Now, it becomes believable that under the normalization $q_1 = 1$, the q_j 's

nearest zero appear to become evenly distributed, while the larger values demonstrate a stretch/pull phenomenon that is still not understood. In the limit, the end of $M_{p,k}$ appears to be pushed to infinity, and the handles become evenly distributed along the x_3 -axis. This suggests the following conjecture.

Conjecture 5.1. *If $M_{p,k}$ exists for all $p > 0$ and $k > 2$, then, for fixed k and $p \rightarrow \infty$, with a homothety normalization, the surfaces $M_{p,k}$ converge to the Karcher saddle tower [Karcher 1988] with normal rotational symmetry of order k .*

We cannot prove this conjecture. However, assuming it to be true, we were led to the correct Weierstrass data for the saddle towers viewed as complete surface in \mathbb{R}^3 of infinite genus, which we explain in Section 6. The critical observations in this process were: first, that the conjecture implied that the values q_j , which solve the period problem $S_{p,k}$, become equidistant along the real axis as p gets large; second, that the algebraic equation for the underlying Riemann surface $M_{p,k}$ then becomes a truncation to the first $2p + 1$ terms of the infinite product expansion for $\tan z$. Based on these observations, we started the period calculations for $S_{p,k}$ for $p \geq 400$, with initial data $q_j = j$. In so doing, we observed that the periods nearest the point 0 are nearly zero, while those far from this point can be quite large.

6. A GLOBAL REPRESENTATION OF KARCHER'S SADDLE TOWERS

Scherk's original paper [1835] announced the existence of a family of *singly periodic* embedded minimal surfaces. Taking the periodic direction to be vertical, one can think of Scherk's examples as a minimal desingularization of two planes in \mathbb{R}^3 meeting along the x_3 -axis. See Figure 10 (left).

This heuristic suggested to H. Karcher a generalization of Scherk's surfaces that desingularizes k planes in \mathbb{R}^3 , all meeting along the x_3 -axis, for $k \geq 3$. He succeeded [Karcher 1988] in constructing

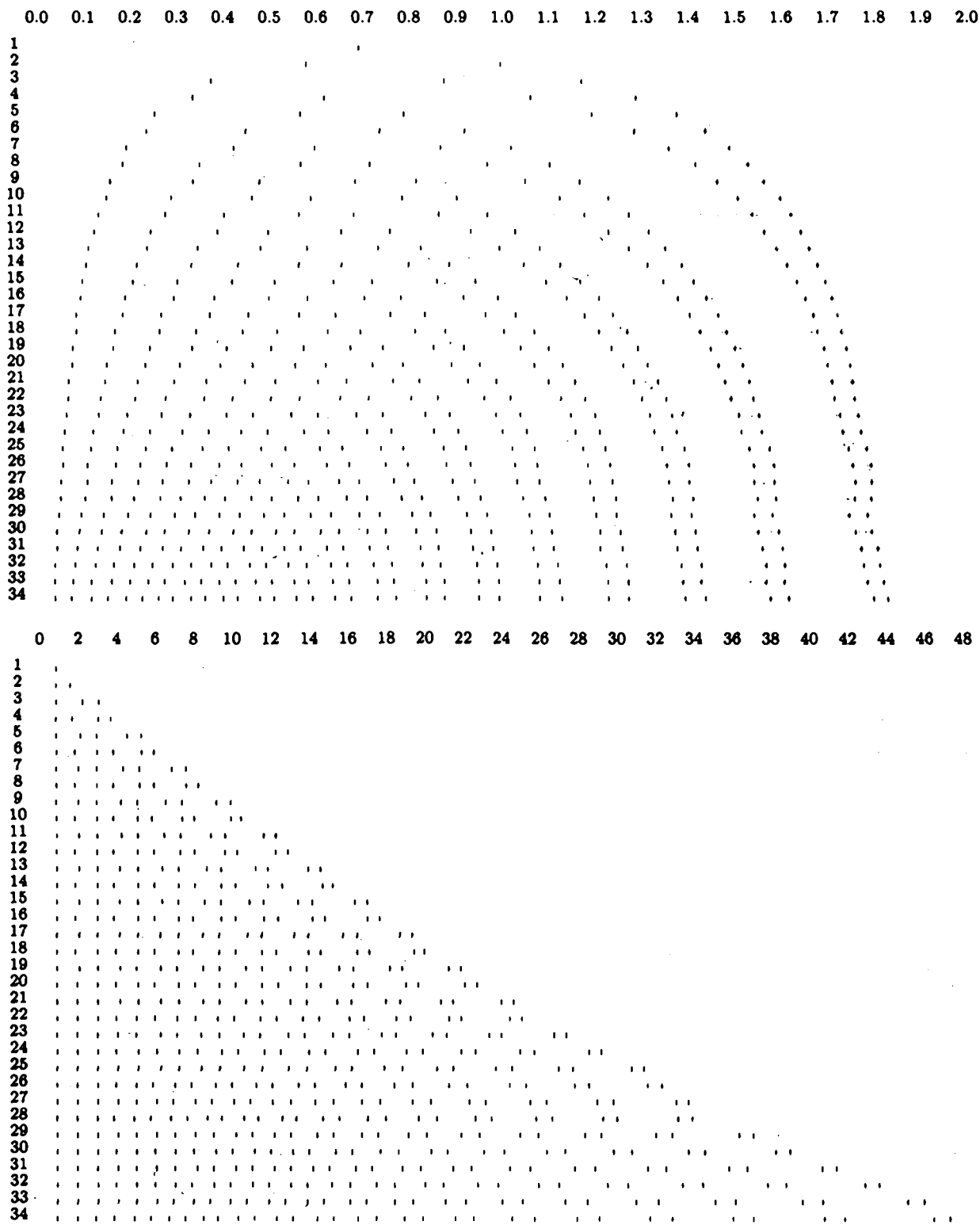


FIGURE 9. Period solutions for $M_{p,2}, p = 1, 2, \dots, 34$. Top: normalization $B = 1$. Bottom: normalization $q_1 = 1$.

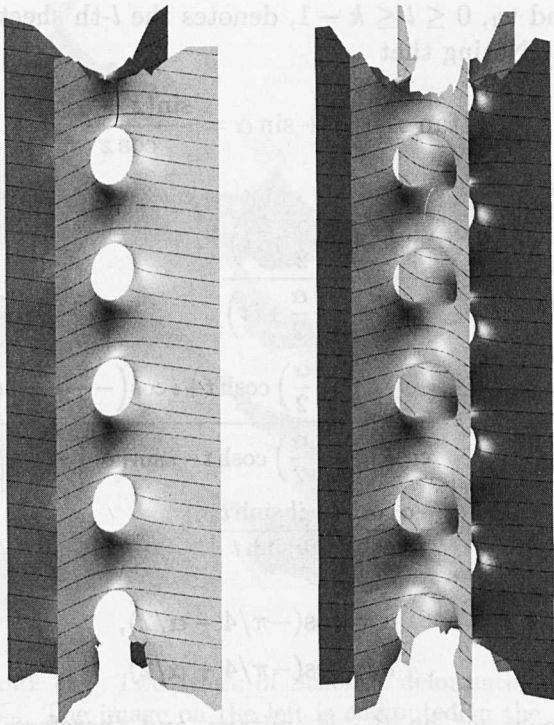


FIGURE 10. Karcher saddle towers drawn from global data for $k = 2$ (left), and 3, (right) with $\alpha = 0$ or $\varphi = \pi/(2k)$.

these surfaces, which he called *saddle towers*, and which we denote here by $S_{k,\varphi}$, for $0 < \varphi \leq \pi/(2k)$. See Figure 10 (right) for an image of $S_{3,\pi/(2k)}$.

Two nonparallel planes in \mathbb{R}^3 can be completely described, up to Euclidean motion, by the angle between them, which we take as the parameter for Scherk’s family. Given k planes, $k \geq 3$, with a common line of intersection, there are more possibilities. The first case considered by Karcher is the maximally symmetric one, where the angle between successive half-planes equals π/k . These saddle towers are called *symmetric*, and we denote them here by $S_{k,\pi/(2k)}$. A *wing* of a saddle tower is the portion of the surface asymptotic to a half plane. Our notation is chosen because these surfaces have $2k$ planar reflectional symmetries, one between each pair of successive wings, and we measure the angle from these planar geodesics. On $S_{k,\pi/(2k)}$, the limit normals to the wings are the

horizontal vectors whose stereographic projections equal $i\xi$, where $\xi^{2k} = 1$.

Karcher generalized these examples by constructing the surfaces $S_{k,\varphi}$, for $0 < \varphi < \pi/(2k)$, where this angle is changed so that the limit normals are $e^{\pm i\varphi}\xi$. We refer to the $S_{k,\varphi}$ as *symmetrically deformed saddle towers*. For some values of φ , these surfaces are no longer embedded.

Since $S_{k,\varphi}$ is singly periodic and nonflat, it has infinite total curvature. But, by factoring \mathbb{R}^3 by the translational symmetry of $S_{k,\varphi}$, one produces a minimal surface of finite total curvature in $\mathbb{R}^2 \times S^1$. On this surface, Karcher assumed a planar reflectional symmetry corresponding to inversion of the Gauss map through the unit circle. He also assumed that the fundamental domain of this reflection had $2k$ distinct planes of reflectional symmetry that meet along the vertical axis. This axis intersects the surface at the saddle points. The order-preserving symmetries generated by these reflections form a normal rotational symmetry of order k around this axis.

Using these symmetries and the end behavior, Karcher determined the data for $S_{k,\varphi}$ to be

$$g = \xi^{k-1}, \quad \varphi_3 = \frac{1}{\xi^k + \xi^{-k} - 2\cos(k\varphi)} \frac{d\xi}{\xi}, \quad (6.1)$$

where $0 < \varphi \leq \frac{\pi}{2k}$.

We now prove the following result:

Theorem 6.1. *Let*

$$M_{k,\alpha} = \{(z, w) \in \mathbb{C} \times \mathbb{P}^1 : w^k = \tan z \cos \alpha + \sin \alpha\},$$

where $\alpha \in [0, \pi/2)$. The mapping $X : M_{k,\alpha} \rightarrow \mathbb{R}^3$ defined by (2.1) with

$$g = w^{k-1}, \quad \varphi_3 = dz \quad (6.2)$$

is a conformal diffeomorphism between $M_{k,\alpha}$ and $S_{k,\varphi}$, where $\alpha = \pi/2 - k\varphi$.

Remark 6.2. The symmetric saddle towers correspond to $\alpha = 0$, so that $M_{k,0}$ is defined by

$$w^k = \tan z = \prod_{l=1}^{\infty} \frac{z^2 - (2l\pi)^2}{z^2 - ((2l-1)\pi)^2}$$

Truncation of this infinite product expansion of the tangent function produces the algebraic equations for $M_{p,k}$. The poles and zeros for this truncation must be adjusted so as to solve the period problem on $M_{p,k}$. Truncations of the general infinite product expansions ($\alpha \neq 0$) have been investigated in the hope of finding new minimal surfaces of finite total curvature that may converge to the $S_{k,\varphi}$. In general, this corresponds to removing the restriction that the q_j be strictly real, allowing them to vary over the entire complex numbers. When the period problems associated with these truncations were fed into the same software used for the periods of $M_{p,k}$, the solutions were observed to converge to values associated with the more symmetric examples $M_{p,k}$ —that is, the q_j approached real numbers as the periods approached zero.

Proof. In order to make a comparison between the two representations (6.1) and (6.2), we restrict the data in (6.2) to

$$B = \left\{ (z, w) \in M_{k,\alpha} : -\frac{\pi}{4} - \frac{\alpha}{2} < \operatorname{Re} z \leq \frac{3\pi}{4} - \frac{\alpha}{2} \right\}.$$

Using basic properties of the tangent function, we see that g on B is a bijective mapping onto $\mathbf{P}^1 \setminus \{w : w^k = ie^{\pm i\alpha}\}$. Comparison of the two Gauss maps suggests the following relationship between ξ and z :

$$\xi = (\tan z \cos \alpha + \sin \alpha)^{1/k}.$$

Performing this change of variable on φ_3 in (6.1), we see that the height differentials differ by a real constant dependent on k and α . Therefore, up to homothety, $X(B)$ is congruent to a fundamental domain of $S_{k,\alpha}$.

We next show that $\partial X(B)$ consists of planar geodesics, from which it follows that $X(M_{k,\alpha})$ and $S_{k,\varphi}$ are congruent. Let $\beta_{j,l} = (\gamma_j(t), w_l(\gamma_j(t)))$, where $\gamma_j(t) = -\pi/4 + j\pi - \alpha/2 + it$, $t \in \mathbf{R}$, $j = 0, 1$,

and w_l , $0 \leq l \leq k-1$, denotes the l -th sheet over γ_j . Noting that

$$\tan z \cos \alpha + \sin \alpha = \frac{\sin(z + \alpha)}{\cos z},$$

we have

$$\begin{aligned} w^k(\gamma_0(t)) &= \frac{\sin\left(-\frac{\pi}{4} + \frac{\alpha}{2} + it\right)}{\cos\left(-\frac{\pi}{4} - \frac{\alpha}{2} + it\right)} \\ &= \frac{\sin\left(-\frac{\pi}{4} + \frac{\alpha}{2}\right) \cosh t + i \cos\left(-\frac{\pi}{4} + \frac{\alpha}{2}\right) \sinh t}{\cos\left(-\frac{\pi}{4} - \frac{\alpha}{2}\right) \cosh t - i \sin\left(-\frac{\pi}{4} - \frac{\alpha}{2}\right) \sinh t} \\ &= \frac{-a \cosh t + ib \sinh t}{a \cosh t + ib \sinh t}, \end{aligned}$$

where

$$a = \cos(-\pi/4 - \alpha/2),$$

$$b = \cos(-\pi/4 + \alpha/2).$$

Hence w^k on $\beta_{0,l}$ is unitary, and therefore so is $g = w^{k-1}$. Therefore $(dg/g)(\beta'_{0,l}) \subset i\mathbf{R}$, so that $\Pi(\beta_{0,l}) \subset \mathbf{R}$. Since the automorphism of $M_{k,\alpha}$ induced by $z \mapsto -\bar{z} - \pi/2 - \alpha$ is an isometry fixing $\beta_{0,l}$, we see that $\beta_{0,l}$ is a geodesic. By Lemma 2.1 it is planar. A similar analysis for $j = 1$ reveals that $g(\beta_{1,l})$ is unitary and $\beta_{1,l}$ is a geodesic.

We have shown that $\partial X(B)$ consists of $2k$ planar geodesics. Extending $X(B)$ across these curves by Schwarz reflection produces a surface that agrees with $X(M_{k,\alpha})$, so $X(M_{k,\alpha})$ is congruent to $S_{k,\varphi}$. This completes the proof. \square

6.1. A Global Representation of Scherk's Doubly Periodic Surfaces

Scherk's 1835 paper also describes a one parameter family of embedded doubly periodic minimal surfaces in \mathbf{R}^3 . Factoring any surface in the family by its two translational symmetries produces a minimal sphere in $T \times \mathbf{R}$ with four points removed, where T is a rhombic torus and the puncture points represent the ends. With the traditional orientation and position of this surface in \mathbf{R}^3 , the stereographic projection of the limit-normals

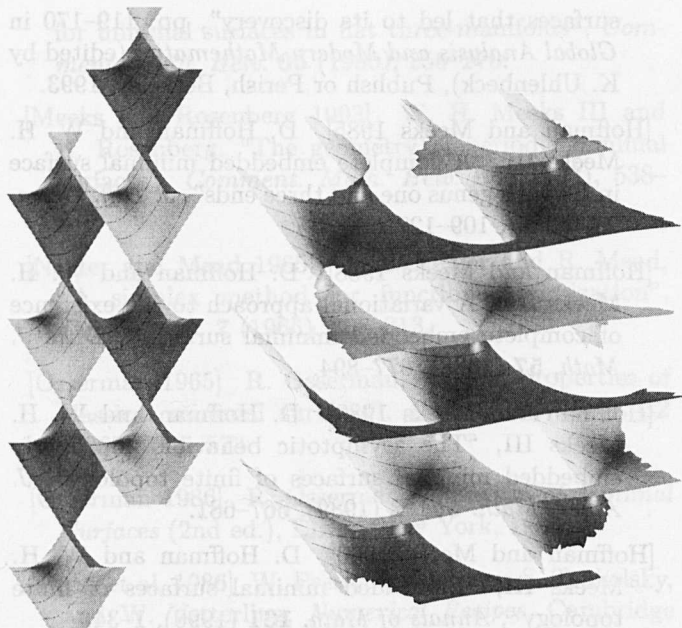


FIGURE 11. Two views of Scherk's deformation of S_0 . The image on the left is computed in the quotient and the one on the right is computed by global data.

at these ends is $\pm e^{\pm i\theta}$, for $\theta \in (0, \pi/4]$. Consecutive 90° rotations about the x_2 and x_3 axes reposition the surface so that the values omitted by the stereographic projection of the Gauss map become $\{0, \infty, \alpha i, -\alpha^{-1}i\}$, with $\alpha \in (0, 1]$. We choose to use α as the deformation parameter, and denote the complete surface in \mathbb{R}^3 by S_α , and its quotient in $T \times \mathbb{R}$ by \tilde{S}_α . In this section we describe the global representation of the surfaces S_α , but first we review its quotient representation.

Since the quotient surface is conformally a sphere with four ends and the Gauss map is injective, we parametrize it by this map. The end behavior, together with the fact that the height differential has no zeros at finite points, determines the height differential up to a nonzero multiplicative complex constant. The absolute value of this factor is chosen to simplify a later calculation and corresponds to a rescaling in \mathbb{R}^3 . The phase of the multiplicative constant is determined to be zero by the behavior of the data along the straight lines on the

surface. Therefore, the Weierstrass data for \tilde{S}_α in $T \times \mathbb{R}$ is

$$g = \xi, \\ \varphi_3 = \frac{\alpha^2 + 1}{2} \frac{d\xi}{(\xi - \alpha i)(\xi + \alpha^{-1}i)},$$

where ξ is the standard coordinate on $\mathbb{C} \setminus \{0, \alpha i, -\alpha^{-1}i\}$. The Weierstrass representation given by this data is multivalued with two linearly independent periods.

Using arguments similar to those used for the saddle towers, we can prove the following result:

Theorem 6.3. S_α is conformally diffeomorphic to

$$M_\alpha := \left\{ (z, w) \in \mathbb{C}^2 : e^w = -i \frac{e^{iz} - \alpha e^{-iz}}{\alpha e^{iz} + e^{-iz}} \right\}$$

via the mapping $X : M_\alpha \rightarrow \mathbb{R}^3$ defined by (2.1), with

$$g = e^w \\ \varphi_3 = dz.$$

When $\alpha = 1$, this data simplifies to $e^w = \tan z$, which corresponds to the most symmetric Scherk surface.

Remark 6.4. With the global representation in this theorem, one sees directly that, as $\alpha \rightarrow 0$, the Weierstrass data converges to

$$M_0 := \{(z, w) \in \mathbb{C}^2 : e^w = -ie^{2iz}\} = \mathbb{P}^1, \\ g = -ie^{2iz}, \\ \varphi_3 = dz,$$

which is the global data for the helicoid [Hoffman et al. 1993; Hoffman and Wohlgemuth].

Osserman [1985] made the following observation:

Proposition 6.5. S_α has infinite genus and one topological end.

Applying the results of M. Heins, we have an alternative proof of this. Let $f : \mathbb{C} \rightarrow \mathbb{C}$ be an analytic function whose zeros are simple and discrete. Heins

[1952] observed that if such a function has at least two zeros, the Riemann surface defined by

$$e^w = f(z)$$

has infinite genus and one end.

Examination of Heins's argument reveals that the same proof applies to the case in which f has discrete simple poles. Hence, together with Theorem 6.3 we have Osserman's result. Given the conformal diffeomorphism presented above, one may follow Osserman's and Heins's arguments in parallel, to see that they are virtually identical.

ACKNOWLEDGEMENTS

We wish to thank Jim Hoffman at the Center for Geometry, Analysis, Numerics, and Graphics, for his help in preparing images.

REFERENCES

- [Bloß 1989] D. Bloß, "Elliptische Funktionen und vollständige Minimalflächen", Ph.D. thesis, Freie Universität Berlin, 1989.
- [Chen and Gackstatter 1982] C. C. Chen and F. Gackstatter, "Elliptische und hyperelliptische Funktionen und vollständige Minimalflächen vom Enneperschen Typ", *Math. Ann.* **259** (1982), 359–369.
- [Callahan et al. 1990] M. Callahan, D. Hoffman, and W. H. Meeks III, "The structure of singly-periodic minimal surfaces", *Inventiones Math.* **99** (1990), 455–481.
- [Espírito Santo 1993] N. do Espírito Santo, "Superfícies mínimas completas em \mathbb{R}^3 com fim de tipo Enneper", Ph.D. thesis, Instituto de Matemática Pura e Aplicada, Rio de Janeiro, 1993.
- [Gackstatter 1976] F. Gackstatter, "Über die Dimension einer Minimalfläche und zur Ungleichung von St. Cohn-Vossen", *Arch. Rational Mech. Anal.* **61**(2) (1976), 141–152.
- [Heins 1952] M. Heins, "Riemann surfaces of infinite genus", *Annals of Math.*, **55** (1952), 296–317.
- [Hoffman et al. 1993] D. Hoffman, H. Karcher, and F. Wei, "The genus one helicoid and the minimal surfaces that led to its discovery", pp. 119–170 in *Global Analysis and Modern Mathematics* (edited by K. Uhlenbeck), Publish or Perish, Berkeley, 1993.
- [Hoffman and Meeks 1985] D. Hoffman and W. H. Meeks III, "A complete embedded minimal surface in \mathbb{R}^3 with genus one and three ends", *J. Diff. Geom.* **21** (1985), 109–127.
- [Hoffman and Meeks 1988] D. Hoffman and W. H. Meeks III, "A variational approach to the existence of complete embedded minimal surfaces", *Duke J. Math.* **57** (1988), 877–894.
- [Hoffman and Meeks 1989] D. Hoffman and W. H. Meeks III, "The asymptotic behavior of properly embedded minimal surfaces of finite topology", *J. Amer. Math. Soc.* **2** (1989), 667–681.
- [Hoffman and Meeks 1990] D. Hoffman and W. H. Meeks III, "Embedded minimal surfaces of finite topology", *Annals of Math.* **131** (1990), 1–34.
- [Hoffman 1982] D. Hoffman, review of [Chen and Gackstatter 1982], *Math. Reviews*, 1982. Review number 84d:53005.
- [Hoffman and Wohlgemuth] D. Hoffman and M. Wohlgemuth, "Limiting behavior of classical periodic minimal surfaces", in preparation.
- [Jorge and Meeks 1983] L. Jorge and W. H. Meeks III, "The topology of complete minimal surfaces of finite total Gaussian curvature", *Topology* **22** (1983), 203–221.
- [Karcher 1988] H. Karcher, "Embedded minimal surfaces derived from Scherk's examples", *Manuscripta Math.* **62** (1988), 83–114.
- [Karcher 1989] H. Karcher, "Construction of minimal surfaces", pp. 1–96 in *Surveys in Geometry*, University of Tokyo, 1989, and *Lecture Notes* **12**, SFB256, Bonn, 1989.
- [Kusner 1987] R. Kusner, "Conformal geometry and complete minimal surfaces", *Bull. Amer. Math. Soc.* **17** (1987), 291–295.
- [Lopez 1992] F. J. Lopez, "The classification of complete minimal surfaces with total curvature greater than -12π ", *Trans. Amer. Math. Soc.* **334** (1992), 49–74.
- [Meeks and Rosenberg 1990] W. H. Meeks III and H. Rosenberg, "The maximum principle at infinity

- for minimal surfaces in flat three-manifolds”, *Comment. Math. Helv.* **65** (1990), 255–270.
- [Meeks and Rosenberg 1993] W. H. Meeks III and H. Rosenberg, “The geometry of periodic minimal surfaces”, *Comment. Math. Helv.* **68** (1993), 538–578.
- [Nelder and Mead 1965] J. A. Nelder and R. Mead, “A simplex method for function minimization”, *Computer J.* **7** (1965), 308–313.
- [Osserman 1965] R. Osserman, “Global properties of classical minimal surfaces”, *Duke J. of Math.* **32** (1965), 565–573.
- [Osserman 1986] R. Osserman, *A Survey of Minimal Surfaces* (2nd ed.), Dover, New York, 1986.
- [Press et al. 1986] W. Press, B. Flannery, S. Teukolsky, and W. Vetterling, *Numerical Recipes*, Cambridge University Press, Cambridge, 1986.
- [Scherk 1835] H. F. Scherk, “Bemerkungen über die kleinste Fläche Innerhalb gegebener Grenzen”, *J. reine angew. Math.* **13** (1835), 185–208.
- [Schoen 1983] R. Schoen, “Uniqueness, symmetry, and embeddedness of minimal surfaces”, *J. Diff. Geom.* **18** (1983), 791–809.
- [Traizet] M. Traizet, “New triply periodic minimal surfaces”, preprint III.22, GANG, University of Massachusetts, Amherst.
- [Wohlgemuth 1993] M. Wohlgemuth, “Vollständige Minimalflächen höheren Geschlechts und endlicher Totalkrümmung”, Ph.D. thesis, University of Bonn, 1993.

Software Availability

The code for solving the period problem is available in the form of a C++ function that returns the values of q_1, q_2, \dots, q_p given $p \leq 34$ and some values of k . Send requests to the author at ed@gang.umass.edu.

The program MESH, created by Jim Hoffman, was used to generate all the surfaces shown. MESH is available by anonymous ftp from <ftp.gang.umass.edu>, in directory `pub/mesh`. Questions concerning this distribution should be directed to Dave Oliver at mesh_help@gang.umass.edu.

Edward C. Thayer, Department of Mathematics, University of Massachusetts, 1535 Lederle Graduate Research Center Towers, Amherst, MA 01003

Received November 7, 1994; accepted in revised form March 21, 1995